Surface ozone-temperature relationships in the eastern US: A monthly climatology for evaluating chemistry-climate models

D.J. Rasmussen [a,*,1], A.M. Fiore [a,2], V. Naik [b], L.W. Horowitz [a], S.J. McGinnis [c], M.G. Schultz [d]

[a] Geophysical Fluid Dynamics Laboratory (GFDL), National Oceanic and Atmospheric Administration (NOAA), Princeton, NJ 08540, USA
[b] High Performance Technologies Inc./GFDL, NOAA, Princeton, NJ 08540, USA
[c] Department of Geosciences, Princeton University, Princeton, NJ 08544, USA
[d] IEK-8, Forschungszentrum Jülich, Jülich, Germany

ABSTRACT

We use long-term, coincident O_3 and temperature measurements at the regionally representative US Environmental Protection Agency Clean Air Status and Trends Network (CASTNet) over the eastern US from 1988 through 2009 to characterize the surface O_3 response to year-to-year fluctuations in weather, for the purpose of evaluating global chemistry-climate models. We first produce a monthly climatology for each site over all available years, defined as the slope of the best-fit line (m_{O3-T}) between monthly average values of maximum daily 8-hour average (MDA8) O_3 and monthly average values of daily maximum surface temperature (T_{max}). Applying two distinct statistical approaches to aggregate the site-specific measurements to the regional scale, we find that summer time m_{O3-T} is 3–6 ppb K^{-1} ($r = 0.5$ –0.8) over the Northeast, 3–4 ppb K^{-1} ($r = 0.5$–0.9) over the Great Lakes, and 3–6 ppb K^{-1} ($r = 0.2$–0.8) over the Mid-Atlantic. The Geophysical Fluid Dynamics Laboratory (GFDL) Atmospheric Model version 3 (AM3) global chemistry-climate model generally captures the seasonal variations in correlation coefficients and m_{O3-T} despite biases in both monthly mean summertime MDA8 O_3 (up to +10 to +30 ppb) and daily T_{max} (up to +5 K) over the eastern US. During summer, GFDL AM3 reproduces m_{O3-T} over the Northeast ($m_{O3-T} = 2$–6 ppb K^{-1}; $r = 0.6$–0.9), but underestimates m_{O3-T} by 4 ppb K^{-1} over the Mid-Atlantic, in part due to excessively warm temperatures above which O_3 production saturates in the model. Combining T_{max} biases in GFDL AM3 with an observation-based m_{O3-T} estimate of 3 ppb K^{-1} implies that temperature biases could explain up to 5–15 ppb of the MDA8 O_3 bias in August and September though correcting for excessively cool temperatures would worsen the O_3 bias in June. We underscore the need for long-term, coincident measurements of air pollution and meteorological variables to develop process-level constraints for evaluating chemistry-climate models used to project air quality responses to climate change.

Published by Elsevier Ltd.

1. Introduction

Surface ozone (O_3) is a secondary pollutant that is produced by the photochemical oxidation of carbon monoxide (CO), methane (CH$_4$), and non-methane volatile organic compounds (NMVOCs) by OH in the presence of nitrogen oxides (NO$_x$ ≡ NO + NO$_2$). As surface O_3 is a public health concern (Bernard et al., 2001; Levy et al., 2001), air quality managers seek to be informed as to how surface O_3 will evolve in the future. Chemistry-climate models (CCMs) are increasingly being applied to project air quality under various global change scenarios, but model biases in representing present-day meteorology and chemical environments raise concern as to their ability to project accurately the response of air pollution to changes in climate and emissions (Fiore et al., 2009; Murazaki and Hess, 2006; Reidmiller et al., 2009). Here we assess the capability of a CCM to represent the surface O_3 response to interannual variations in temperature. In contrast to many prior studies which compare simulated and observed O_3 or temperature individually, we hypothesize that this more process-oriented evaluation of CCM representation of the surface O_3 response to changes in average temperatures is more relevant to assessing model skill at projecting the O_3 response to climate change. Similar mechanistic air quality model evaluation approaches have

* Corresponding author.
 E-mail address: david.rasmussen@noaa.gov (D.J. Rasmussen).
 [1] Now at Department of Civil and Environmental Engineering, University of California, Davis, CA 95616, USA.
 [2] Now at Lamont-Doherty Earth Observatory, Columbia University, Palisades, NY 10964, USA.

previously been applied to gauge the O_3 response to simulated NO_x emission reductions over the eastern US (Gilliland et al., 2008; Godowitch et al., 2008).

Observational studies indicate strong correlation between surface temperature and O_3 concentrations on multiple time scales (Bloomer et al., 2009; Camalier et al., 2007; Cardelino and Chameides, 1990; Clark and Karl, 1982; Korsog and Wolff, 1991), including between monthly average O_3 and monthly average temperatures in the warm season over the eastern US (Lin et al., 2001; National Research Council (U.S.). Committee on Tropospheric Ozone Formation and Measurement, 1991). A warming climate is expected to exacerbate O_3 pollution in densely populated regions of the US, such as over the Northeast where climate models consistently show annual temperature increases of at least 2 K over the 21st century (Christensen et al., 2007), possibly offsetting the benefits from emissions reductions, increasing the number of high-O_3 days, and lengthening the O_3 season (Bloomer et al., 2010; Hogrefe et al., 2004; Jacob and Winner, 2009; Kunkel et al., 2008; Murazaki and Hess, 2006; Nolte et al., 2008; Racherla and Adams, 2006; Wu et al., 2008). This "climate change penalty" has been previously defined equivalently within the context of both O_3 and NO_x: (a) the reduced benefits of emission controls due to the increase in O_3 in a warmer climate; (b) the additional decreases in NO_x emissions needed to counter any climate-induced increase in O_3 in order to meet established air quality goals, under the assumption that NO_x is the limiting precursor for O_3 formation (Wu et al., 2008).

Temperature is a useful proxy to synthesize the complex effects of meteorological and chemical factors influencing O_3 concentrations. Over the eastern United States, these effects, expressed as the total derivative ($d[O_3]/dT$), reflect at least three components:

$$d[O_3]/dT = (1)\partial[O_3]/\partial[\text{stagnation}]*\partial[\text{stagnation}]/\partial T$$
$$+ (2)\partial[O_3]/\partial[\text{PAN}]*\partial[\text{PAN}]/\partial T$$
$$+ (3)\partial[O_3]/\partial[\text{isoprene}]*\partial[\text{isoprene}]/\partial T + \cdots$$

(1) association of warm temperatures with stagnant air masses enabling accumulation of local chemistry precursors that feed O_3 formation in the planetary boundary layer (Jacob et al., 1993; Leibensperger et al., 2008; Olszyna et al., 1997); (2) thermal decomposition of peroxyacetylnitrate (PAN) at high temperatures, thus decreasing NO_x and HO_x sequestration at low temperatures (Cardelino and Chameides, 1990; Sillman and Samson, 1995); and (3) increasing biogenic emissions of isoprene, an abundant and highly reactive NMVOC precursor for O_3 formation under high-NO_x conditions (Guenther et al., 1993; Lamb et al., 1987; Meleux et al., 2007). In addition, both anthropogenic and natural emissions of NO_x may increase with temperature (Brühl and Crutzen, 1988; Logan, 1983; Yienger and Levy, 1995), and from wildfires in the western US (Jaffe, 2011). The sign of other temperature dependent processes is less certain as they have shown regionally variable effects on O_3 concentrations. These include humidity in the Mid-Atlantic (generally negative over rural areas, but mixed effects over polluted regions) (Camalier et al., 2007; Davis et al., 2011; Dawson et al., 2007) and mixing depths in southern California (little effect) (Aw and Kleeman, 2003) and in the eastern US (positive ozone dependency on mixing depth in low ozone regions and vice-versa) (Dawson et al., 2007). Here we focus on $d[O_3]/dT$, which can be determined from available long-term meteorology and underscore a need for future work to identify observed constraints on the individual processes (partial derivatives) contributing to $d[O_3]/dT$.

Past studies have found $d[O_3]/dT$ to be approximately linear over the temperature range of 290–305 K (Bloomer et al., 2009; Camalier et al., 2007; Mahmud et al., 2008; Sillman and Samson, 1995). The slope of this linear relationship, hereafter m_{O3-T}

(Steiner et al., 2010), has been referred to as the "climate change penalty factor" (Bloomer et al., 2009) in reference to the increase in O_3 associated with increasing temperature. Using historically observed relationships for projecting future changes assumes stationarity in chemical environments (e.g. emissions of both anthropogenic and biogenic origin) and neglects known complex chemistry-weather feedbacks (Lin et al., 1988; National Research Council (U.S.). Committee on Tropospheric Ozone Formation and Measurement, 1991; Steiner et al., 2006; Weaver et al., 2009). Significant spatial and temporal variability in the O_3-temperature relationship occurs across the eastern US due to variations in chemical and meteorological environments that strongly influence surface O_3 formation (Bloomer et al., 2010; Camalier et al., 2007; Jacob et al., 1995; Klonecki and Levy, 1997). While these relationships will evolve with future changes in emissions and climate, we suggest that the ability of a model to resolve these present-day relationships is a useful first test to build confidence in its application for projecting future air quality responses to climate change.

Since a global CCM is expected to resolve synoptic, though not local, scales (e.g. Fiore et al., 2003), we construct monthly, site-level and regional O_3-temperature climatologies from the US Clean Air Status and Trends Network (CASTNet) in the eastern US (Sections 2 and 3) where pollution episodes are large-scale (Logan, 1989) and observational records are longest. We note that differences between urban and rural O_3-temperature sensitivities (Sillman and Samson, 1995) may complicate characterization of broad spatial patterns in these relationships. These observation-based climatologies are then used to evaluate the GFDL AM3 CCM (Sections 2 and 4) and further applied to quantify any contribution from AM3 temperature biases in the eastern US to the summertime AM3 O_3 bias (Section 5), which has also been noted in present day regional (Nolte et al., 2008) and global (Fiore et al., 2009; Murazaki and Hess, 2006; Reidmiller et al., 2009) chemical transport models, before concluding (Section 6).

2. Datasets and statistical approach

2.1. CASTNet observations

Operating since 1987, the CASTNet (Clarke et al., 1997) is an observational network that is spatially designed to be regionally representative of rural conditions,[3] potentially more suitable to compare with a coarse horizontal resolution (in this case, roughly 2°) global climate model than other available datasets. The CASTNet measures both pollutants and weather variables; we use co-located, hourly surface O_3 and temperature. Temperature is at 2-m, measured with platinum resistance (accuracy, ±0.5 K; precision, ±1.0 K) and O_3 with ultra-violet absorbance (accuracy and precision, ±10%).[4] We use monthly mean maximum daily surface temperature (hereafter denoted as $T_{\max}$) and monthly mean maximum daily 8-hour average (MDA8) O_3 calculated from hourly observations, requiring at least 20 days of data per month. Each of these 20 days must have at least 18 hourly temperature and O_3 values in addition to 6 out of 8 hourly O_3 observations to calculate an 8-hour O_3 average. The choice of monthly mean values reflects our focus on inter-annual variability, which should be more relevant to evaluating model O_3 responses to shifts in climate (average weather) rather than to synoptic or diurnal variability.

---

[3] EPA, CASTNet Facts Sheet; http://epa.gov/castnet/javaweb/docs/CASTNET_factsheet_2007.pdf.

[4] EPA, CASTNet Quality Assurance, 3rd Quarterly Report, 2010; http://epa.gov/castnet/javaweb/docs/QA_Quarterly_2010_Q3.pdf.
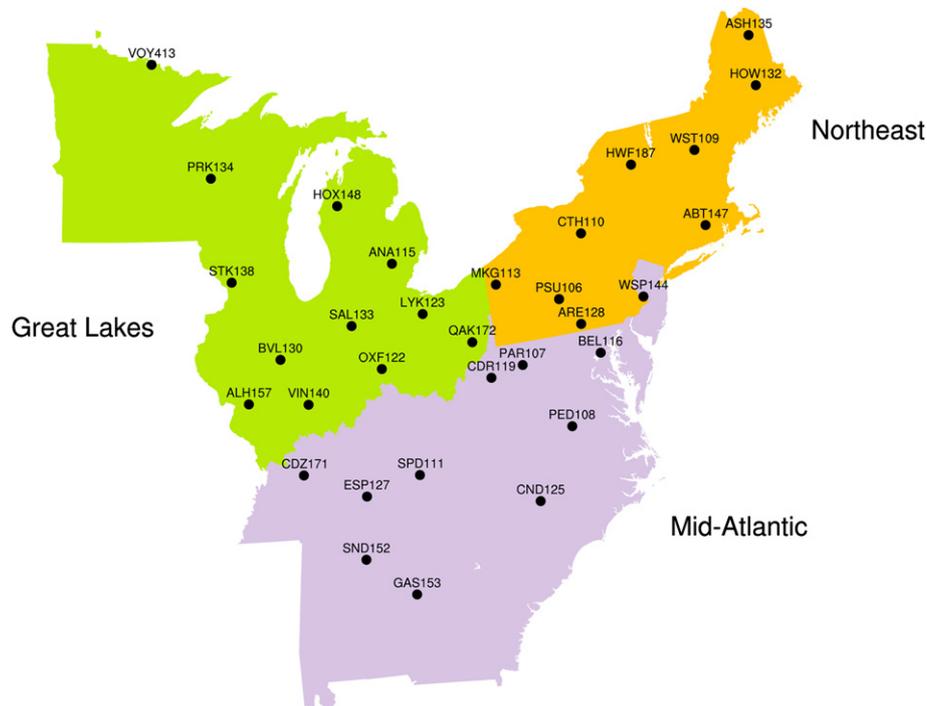
Fig. 1. Geographic locations of CASTNet observation sites in three eastern US regions: Great Lakes, Northeast, and the Mid-Atlantic where all site selection criteria are met (Section 2). All sites have at least seven years of data from 1988—2009; all sites reside at elevations greater than 2 m and less than 600 m; all sites are at least 50 km from oceanfront; when more than one CASTNet site lies within a model grid box, the site with the longest record is used.

2.2. Model description

The GFDL AM3 CCM includes fully coupled stratospheric and tropospheric (both aerosol and NO_x-hydrocarbon-O_3) chemistry and aerosol-cloud interactions within a general circulation model (GCM). As described by Donner et al. (2011), AM3 includes several new physical parameterizations relative to the previous generation (AM2) models and is coupled to a land model (LM3) that includes dynamic vegetation and hydrology (Shevliakova et al., 2009). The tropospheric chemistry and stratospheric chemistry derive from MOZART-2 (Horowitz et al., 2003) and AMTRAC (Austin and Wilson, 2006), respectively, as described by Naik et al. (in preparation) who evaluate global trace gas distributions over recent decades with in situ measurements.

The dynamical core for AM3 is finite-volume, implemented on a cubed sphere (Putman and Lin, 2007). The native cubed sphere grid is C48 horizontal resolution (48×48 cells per face, with the size of the grid cell ranging from ~ 163 km at the corners to ~ 231 km near the face centers) and 48 vertical layers (top level centered at 1.7 Pa). We analyze simulated hourly surface O_3 and temperature fields that have been re-gridded to a latitude-longitude grid with $2° \times 2.5°$ horizontal resolution.

Our simulation follows the specifications for the GFDL AM3 "AMIP" simulations for CMIP5 as described by Donner et al. (2011), except for interactive isoprene emissions as described below. Briefly, AM3 is driven with observed sea surface temperatures and sea ice (Rayner et al., 2003) and aerosol and O_3 precursor emissions from the Atmospheric Chemistry and Climate Model Intercomparison Project (ACCMIP) historical dataset (Lamarque et al., 2010). Thus, we do not expect the model to correspond to the actual synoptic meteorology during the simulation period; certain aspects of interannual variability (those not forced by sea surface temperatures) will not be captured by the model. Greenhouse gas concentrations are set to spatially uniform values for radiation (Meinshausen et al., 2011); for chemically reactive species, those

values are additionally applied as lower boundary conditions. We conduct a 21-year simulation from 1981—2000 and analyze results from 1981—2000 to allow for a one-year initialization. At the time of the simulations, ACCMIP emissions reflecting the NO_x emission reductions between the late 1990s and early 2000s (Frost et al., 2006) were not yet available so we focus on the period where emissions were relatively constant, and year-to-year variability in the model can be attributed largely to changes in average weather and associated feedbacks. Indeed, we find little change in eastern US (bounded by $60° W—95° W$ and $25° N—50° N$) surface anthropogenic NO_x emissions over this period, with annual emissions of 4.23, 4.40, and 4.29 Tg N yr^{-1} in 1980, 1990, and 2000, respectively. Given the small magnitude of these changes, we expect the O_3-temperature relationship to reflect weather variability in the model over these two decades rather than the O_3 response to changes in NO_x emissions.

In order to allow isoprene emissions to respond to fluctuations in solar radiation and temperature, and thereby represent a potentially important positive feedback that enhances O_3 levels in warmer years, we implement a version of Model of Emissions of Gases and Aerosols from Nature (MEGAN) (Guenther et al., 2006), following the approach used in MOZART-4 (Emmons et al., 2010). Emission capacities for five vegetation types are included (version 2.1). Global distributions of 17 plant functional types (PFT) and corresponding leaf area index are based on AVHRR and MODIS data, as used in the NCAR Community Land Model (CLM) (Lawrence and Chase, 2007) and mapped to the five MEGAN vegetation types (see Table 8 of Emmons et al., 2010). Note that these vegetation types and leaf area indices are independent of those within the LM3 dynamic vegetation model. Our implementation uses the model surface air temperature and downward short-wave visible radiation flux each time step, and also includes a dependence on the observed climatological surface air temperature and total downward solar radiation from the previous month. These climatological fields are taken from Sheffield et al. (2006) and are averaged from 1980 to 2000 separately for each
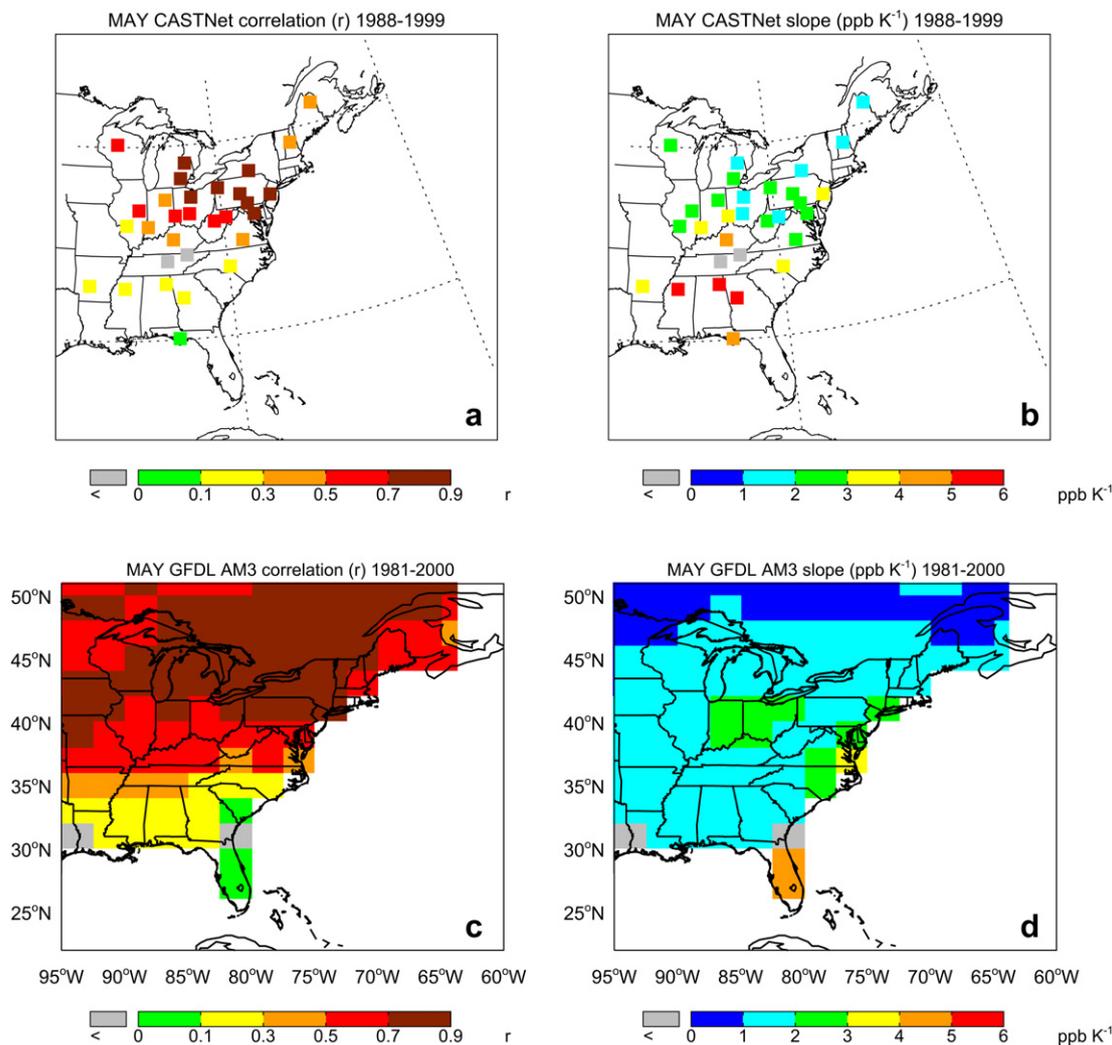
Fig. 2. Pearson correlation coefficient (r) of monthly mean surface MDA8 O_3 (ppb) and monthly mean daily maximum surface temperature (K) over all years from a) individual CASTNet sites (1988−1999) and c) in the GFDL AM3 CCM (1981−2000) in May. The slope of the best-fit line between monthly mean MDA8 O_3 and monthly mean daily maximum surface temperature (m_{O3-T}; ppb K^{-1}) from b) individual CASTNet sites and d) in the GFDL AM3 CCM; all CASTNet sites have at least 7 years of data; grey cells denote where m_{O3-T} minus twice the standard error is less than zero and where modeled m_{O3-T} is less than zero.

month. Annual isoprene emissions for our 1981−2000 period range from 368−405 Tg C globally, and 16−23 Tg C within the United States. The only other emissions tied to the model meteorology are lightning NO_x, but these should have minimal influence in eastern US surface air (Fang et al., 2010).

2.3. Statistical approach

We characterize monthly O_3-temperature relationships by: (1) Pearson correlation coefficients (r) and (2) the slope of the regression line (m_{O3-T}) calculated from monthly mean T_{max} and monthly mean MDA8 O_3 from the CASTNet sites and the GFDL AM3 CCM. The Spearman's rank correlation (Wilks, 2006), a non-parametric statistic (i.e. does not assume Gaussian characteristics), for all correlation analyses yielded little numerical difference from the Pearson correlation coefficients. For calculating m_{O3-T}, we use the reduced major axis (RMA) method, ideally suited for the presence of measurement uncertainties in both x- and y- variables (Ayers, 2001; Cantrell, 2008; Davis, 1986). Unless otherwise noted, all observed data are from 1988−1999, prior to the implementation of the NO_x control SIP Call to avoid aliasing the impacts of NO_x emission changes on O_3 into our estimate of the O_3 response to

temperature (Frost et al., 2006; Gego et al., 2008; Gego et al., 2007). Since NO_x emissions change little in the AM3 simulation (Section 2.2), we use the full 20 years (1981−2000).

In order to be included in our analysis, we require that individual sites meet several conditions: (1) site elevation must be below 600 meters to avoid including free tropospheric air that is not representative of surface conditions (Wunderli and Gehrig, 1991), (2) sites must be approximately 50 km from oceanfront to remove local land-sea meteorological effects, and (3) sites must have data record lengths of at least seven years for each of the three periods we analyze: 1988−1999, 2000−2009, or 1988−2009. We sample the model at the grid box that contains the site latitude and longitude. When more than one site falls within the same model grid box, the site with the longest observational record is used. We then estimate monthly O_3-temperature relationships using three different groupings of monthly mean observations at the sites meeting our selection criteria across all available years: (1) at individual CASTNet sites over the period of 1988−1999; (2) aggregating the valid data under approach (1) into three regions (Fig. 1); and (3) regionally averaged across all sites in Fig. 1 for each year when at least 75% of the sites within the region report valid data and meet our selection criteria. Site groupings for the regional scale

estimates are motivated by past statistical analyses (Chan, 2009; Eder et al., 1993; Lehman et al., 2004).

3. Observed monthly climatologies of the MDA8 O_3-T_{max} relationship

3.1. Climatology for individual CASTNet sites in May and July

We begin by assessing the relationships between MDA8 O_3 and T_{max} at individual CASTNet sites. Here we limit our evaluation to two months during the eastern US O_3 season: (1) May, during which we expect a seasonal transition in the photochemical environment controlling O_3 formation (e.g. changing solar zenith angles, photolysis rates, humidity, and biogenic VOC emissions) (Jacob et al., 1995; Kleinman, 1991; Klonecki and Levy, 1997) and (2) July, when maximum O_3 concentrations typically occur in the eastern US, (e.g. Bloomer et al., 2010). The O_3-temperature correlations at each CASTNet site meeting the predefined selection criteria (Section 2.3) range from $r < 0$ to $+0.9$ in the Mid-Atlantic and generally increase with latitude to 0.3–0.9 in the Great Lakes and the Northeast regions in May (Fig. 2a). This gradient is consistent with that found for a statistical model built on several meteorological variables (predominantly temperature and relative humidity; see Fig. 2, Davis

et al., 2011). A smaller range of 0.3–0.9 with no latitudinal trend is observed in July over the eastern US (Fig. 3a).

Values of May and July m_{O3-T} across individual CASTNet sites vary over the eastern US, however a smaller range of slopes exists over the Great Lakes and Northeast regions in May ($m_{O3-T} = 1$–3 ppb K^{-1}; Fig. 2b). Observed May and July m_{O3-T} tend to decrease with increasing latitude from 4–6 ppb K^{-1} in the southeastern US to 1–2 ppb K^{-1} in May and 2–3 ppb K^{-1} in July (Fig. 3b) at the Ashland, Maine CASTNet site. This decrease in m_{O3-T} from south to north also is consistent with the findings of Davis et al. (2011). The estimated m_{O3-T} in the northern portion of the domain are more robust in terms of statistical significance as evidenced by the higher correlation coefficients in this region.

3.2. Seasonal variations in regional relationships between MDA8 O_3 and T_{max}

We compile monthly mean MDA8 O_3 and T_{max} across all sites within each region (Fig. 1) to construct regional relationships by month for the Northeast, Mid-Atlantic, and Great Lakes (Fig. 4). We consider two time periods: 1988–1999 as in Figs. 2 and 3, as well as 2000–2009, to examine the impact of the 1998 NO_x State Implementation Plan (SIP) Call which reduced summer time power plant
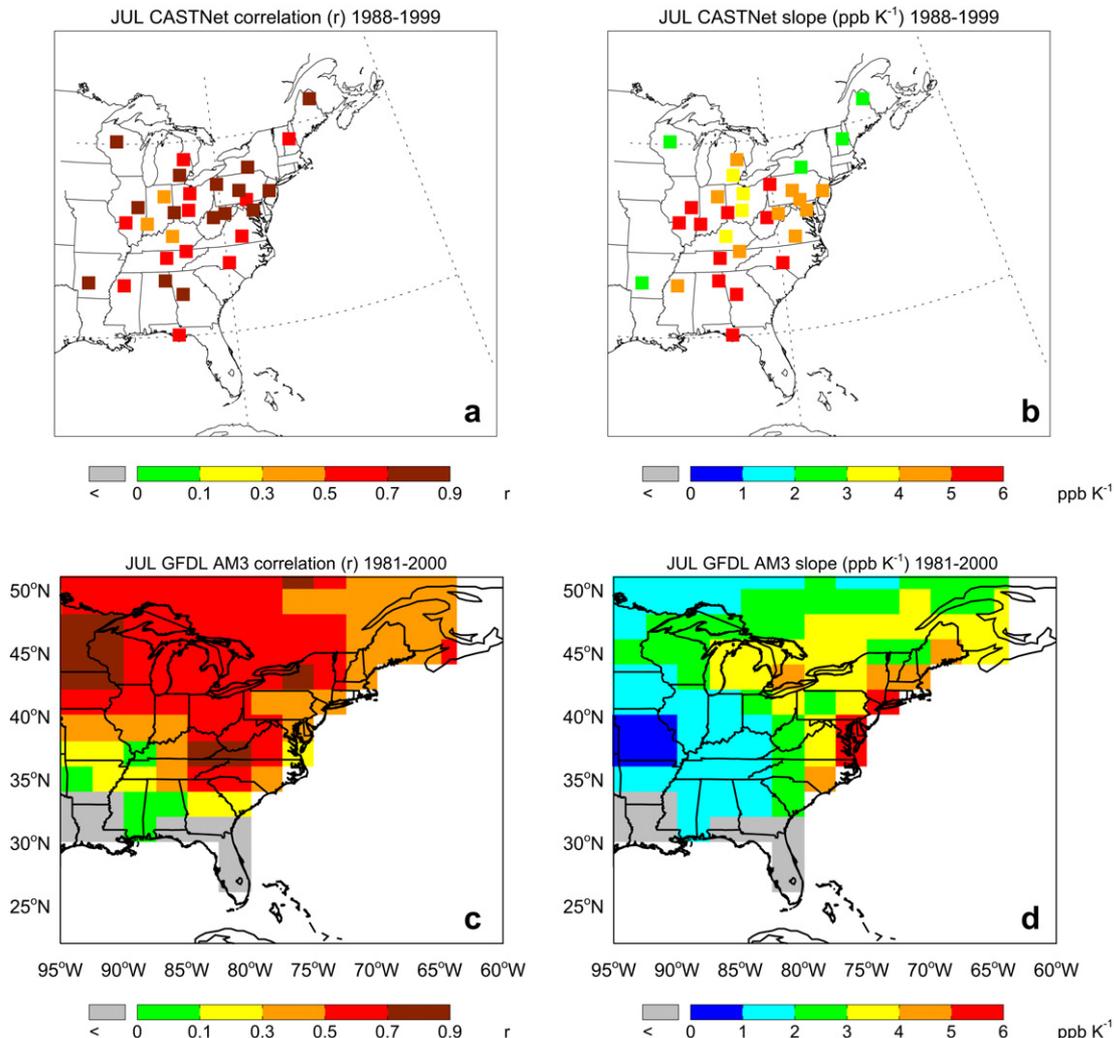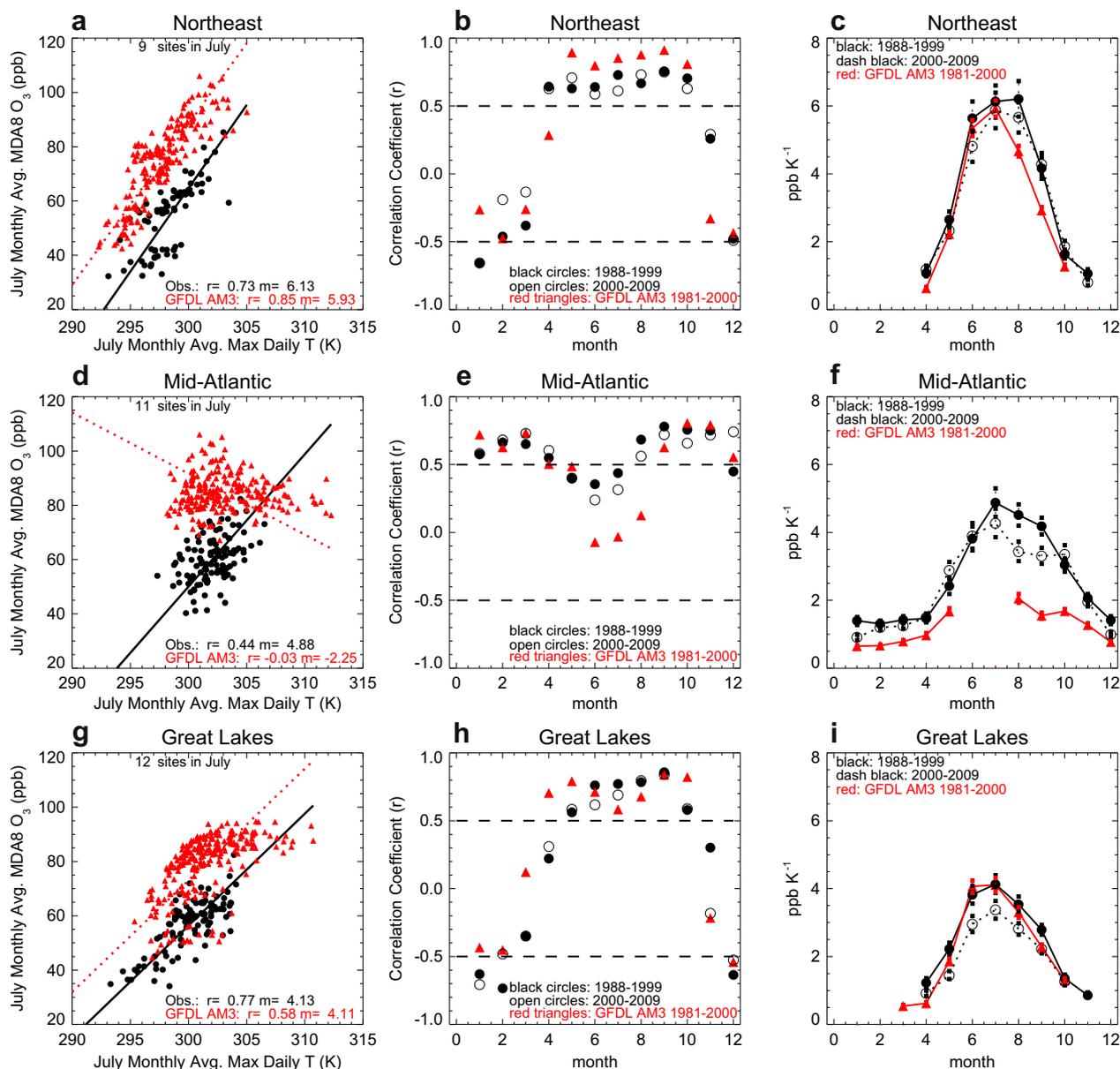

Fig. 3. As for Fig. 2, but for July.

Fig. 4. Relationships between monthly mean surface MDA8 O_3 (ppb) and monthly mean daily T_{max} (K) from all CASTNet site locations in each region for 1988−1999 (solid black circles); 2000−2009 (open black circles); and from the GFDL AM3 model for 1981−2000 (red triangles). Scatter plots of July monthly mean MDA8 O_3 concentration (ppb) and July daily T_{max} (K) with linear regression fits (RMA method; Section 2) representing the corresponding $m_{O3\text{-}T}$ (left column). Also shown are monthly values of Pearson correlation coefficients (r; middle column) and $m_{O3\text{-}T}$ (right column); $m_{O3\text{-}T}$ is not shown for months where $r < 0$; vertical lines indicate ± 1 standard error on $m_{O3\text{-}T}$ (ppb K^{-1}). The dashed lines at $r = \pm 0.5$ indicate where at least 25% of the year-to-year variance in the surface O_3 is associated with temperature variability (For interpretation of the references to color in this figure legend, the reader is referred to the web version of this article.).

emissions in the eastern US by roughly 50% between 1999 and 2003 (Frost et al., 2006).

We first illustrate our approach by estimating $m_{O3\text{-}T}$ for July monthly mean MDA8 O_3 versus July mean T_{max} at each CASTNet site for each year during the period 1988−1999 (Fig. 4). Strong linearity exists between daily T_{max} and MDA8 O_3 over the Northeast ($r = 0.7$; Fig. 4a) and the Great Lakes ($r = 0.8$; Fig. 4g), while a weaker relationship is present in the Mid-Atlantic ($r = 0.4$; Fig. 4d).

Throughout the year we find that O_3-temperature correlations in the Mid-Atlantic (Fig. 4e) are weakest in May, June, and July, ($r < 0.5$) and highest in the autumn, winter, and spring ($r = 0.6$−0.7). In contrast, O_3 and temperature are most strongly correlated in the warmer months in the Northeast (Fig. 4b) and the Great Lakes ($r = 0.6$−0.7; Fig. 4h), and anti-correlated during winter. Hot summer temperatures in the Mid-Atlantic region are

not a reliably strong predictor of high levels of O_3, possibly reflecting offsetting effects of hot and cloudy conditions, a hypothesis previously put forth for the O_3-temperature relationship observed at a site in suburban Georgia (Cardelino and Chameides, 1990). Additionally, summer temperatures in the Mid-Atlantic may regularly exceed the range over which O_3 responds linearly to temperature; this O_3 production "plateau" has been attributed to declining impacts of PAN decomposition at higher temperatures (Steiner et al., 2010).

In all regions, the observed $m_{O3\text{-}T}$ for 1988−1999 has a distinct seasonal cycle, with the highest sensitivities (3−6 ppb K^{-1}) present during the summer and early autumn (Fig. 4c, f, and i). Mean $m_{O3\text{-}T}$ for the O_3 season matches well with the ~ 3 ppb K^{-1} calculated by Bloomer et al. (2009) over the Great Lakes, Northeast, and Mid-Atlantic. Furthermore, we find that a decrease of roughly
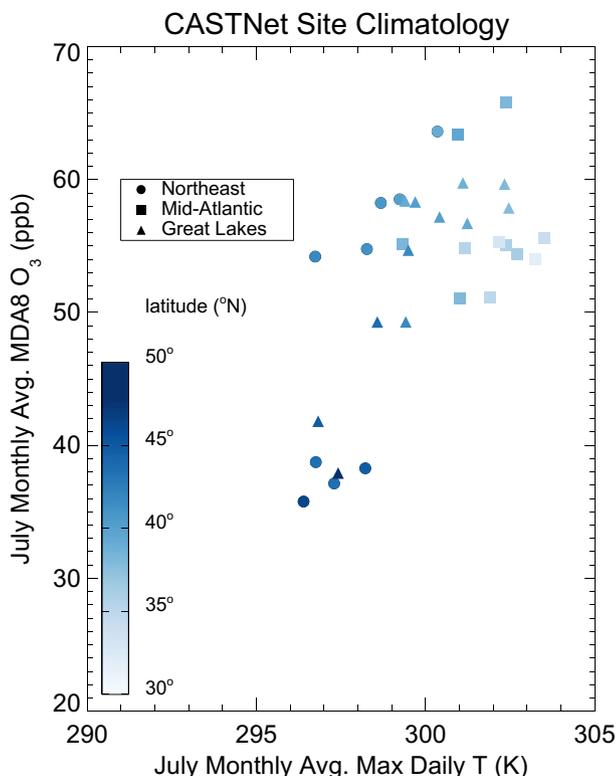
Fig. 5. CASTNet climatology (1988–2009 average) of average July surface MDA8 O_3 (ppb) versus average July daily maximum temperature (K); each symbol corresponds to each CASTNet site from one of the three regions in Fig. 2; circles are Northeast, squares are Mid-Atlantic, and triangles are Great Lakes; shading corresponds to the latitude (°N) of each CASTNet site.

1 ppb K^{-1} in m_{O3-T} during the O_3 season from 1988–1999 to 2000–2009 emerges, consistent with the decrease attributed to the NO_x SIP call emission reductions previously documented (see Fig. 3, Bloomer et al., 2009).

We note an apparent discrepancy between the m_{O3-T} in July in the Northeast (2–6 ppb K^{-1} across the individual CASTNet sites in Fig. 3b) versus the 6 ppb K^{-1} estimate from the regionally aggregated data in Fig. 4c. Since the estimate in Fig. 4c includes data from all the individual sites, we hypothesize that the larger slope reflects the spatial gradients in the O_3 and T_{max} relationship across the region rather than a regionally representative O_3 response to temperature. We next attempt to separate the influence of these spatial gradients from the impact of year-to-year weather fluctuations on O_3. As a first step, we examine climatologies of July monthly mean MDA8 O_3 and T_{max} at CASTNet sites over the eastern US (Fig. 5). We find large variability in the mean July MDA8 O_3 and T_{max} within each of the three regions, including a strong dependence on latitude. In an attempt to filter out this spatial variability, we average the MDA8 O_3 and T_{max} over all CASTNet sites in each region to create regional average records of O_3 and temperature for each month within each year. Averaging only occurs when at least 75% of the sites in each region (Fig. 1) report data for that month. Given the scarcity of temporally coincident observations from sites for the 1988–1999 period, we increase the sample size by expanding to use the full 1988–2009 period. These regionally averaged monthly mean values are then used to estimate m_{O3-T} for each month (Fig. 6). Note that our dataset is shorter than the full 22 year record due to our data screening criteria.

Using this method, the observed m_{O3-T} in the both the Mid-Atlantic and the Great Lakes are within 1 ppb K^{-1} of our estimates when we allow each site to contribute individually to the

O_3-temperature relationship, indicating that the relationships in these regions calculated using the methodology from Fig. 4 primarily reflect the year-to-year variations of MDA8 O_3 with T_{max} which we seek to characterize. For a quantitative comparison between methods (Fig. 4 vs. Fig. 6), the seasonality of m_{O3-T} calculated with observations from 1988–2009 with the methodology used in Fig. 4 is presented as dashed lines (Fig. 6c, f, and i). Over the Northeast, the two methods yield values of m_{O3-T} that differ by up to 2 ppb K^{-1} (solid vs. dashed black lines in Fig. 6c). The lower July sensitivity in Fig. 6c is more consistent with what one would estimate from averaging the values of m_{O3-T} at the individual sites in the Northeast (Fig. 3b). The larger standard errors in Fig. 6 versus Fig. 4 during the warmer months of the year points to a need for longer datasets to improve statistical power.

4. Evaluating modeled monthly climatologies of the MDA8 O_3-T_{max} relationship

Here we evaluate a 20-year simulation with the GFDL AM3 CCM with our observation-derived monthly climatology of O_3-temperature statistics in Section 3. Modeled and observed MDA8 O_3 and T_{max} are compared at individual sites in Figs. 2 and 3. In May, the model (Fig. 2c) captures the broad range of observed correlation coefficients from south to north ($r < 0$ to $+0.9$) over the eastern US (Fig. 2a). North of roughly 37° N, the model reproduces the range of observed m_{O3-T} in May (compare Fig. 2d and b) and generally captures the north-south gradients along the Eastern Seaboard in July (compare Fig. 3d and b) where Camalier et al. (2007) found the highest observed response of O_3 to temperature over the eastern US. The high correlation between O_3 and temperature in summer ($r = 0.3$–0.9) is reproduced by the GFDL AM3 CCM only in the northern half of the domain (Fig. 3c) and m_{O3-T} is underestimated in the Mid-Atlantic US, particularly in the southern and central portions of the region, in May (Fig. 2d) and July (Fig. 3d).

We assess the GFDL AM3 CCM at the regional scale by compiling monthly mean MDA8 O_3 and T_{max} across all grid boxes that contain CASTNet sites to construct regional relationships by month (Fig. 4). Here we compare the model simulation (1981–2000) to the observation period prior to the NO_x SIP Call (1988–1999). We note July O_3 biases of up to $+10$ to $+30$ ppb over all regions (Fig. 4a,d, and g). Summertime O_3 biases over the eastern US have been noted in previous global and regional modeling studies (Fiore et al., 2009; Nolte et al., 2008; Reidmiller et al., 2009). The range of modeled monthly mean T_{max} is also greater than observed at the CASTNet sites in both the Great Lakes and the Mid-Atlantic, with some months exceeding the warmest observed T_{max} by over 5 K. At monthly mean temperatures above 305 K, simulated MDA8 O_3 ceases to respond linearly to increasing T_{max} (Fig. 4d, g). These "plateaus" in MDA8 O_3 may reflect the decreasing lifetime of PAN at incrementally higher temperatures (e.g. Steiner et al., 2010). This saturation effect manifests in the low correlations and slopes noted below for the model.

Over the Northeast and the Great Lakes, the model reproduces the observed correlation coefficients (Fig. 4b, h) and m_{O3-T} (Fig. 4c, i) throughout the year. In the Mid-Atlantic, the AM3 reproduces m_{O3-T} in the winter and early spring and simulates the observed summertime decrease in O_3-temperature correlations, but correlations are excessively weak (July CASTNet: $r = 0.4$; model: $r = 0.0$; Fig. 4e). Additionally, the model underestimates m_{O3-T} in late summer and autumn by as much as 3 ppb K^{-1} (Fig. 4f).

Ideally the model should capture spatial variability in the climatic MDA8 O_3 and T_{max} relationships, which likely results from regional differences in precursor emissions and the photochemical regime, and so we conduct the same comparisons in the model as previously done for the observations in Figs. 4 and 6. We average
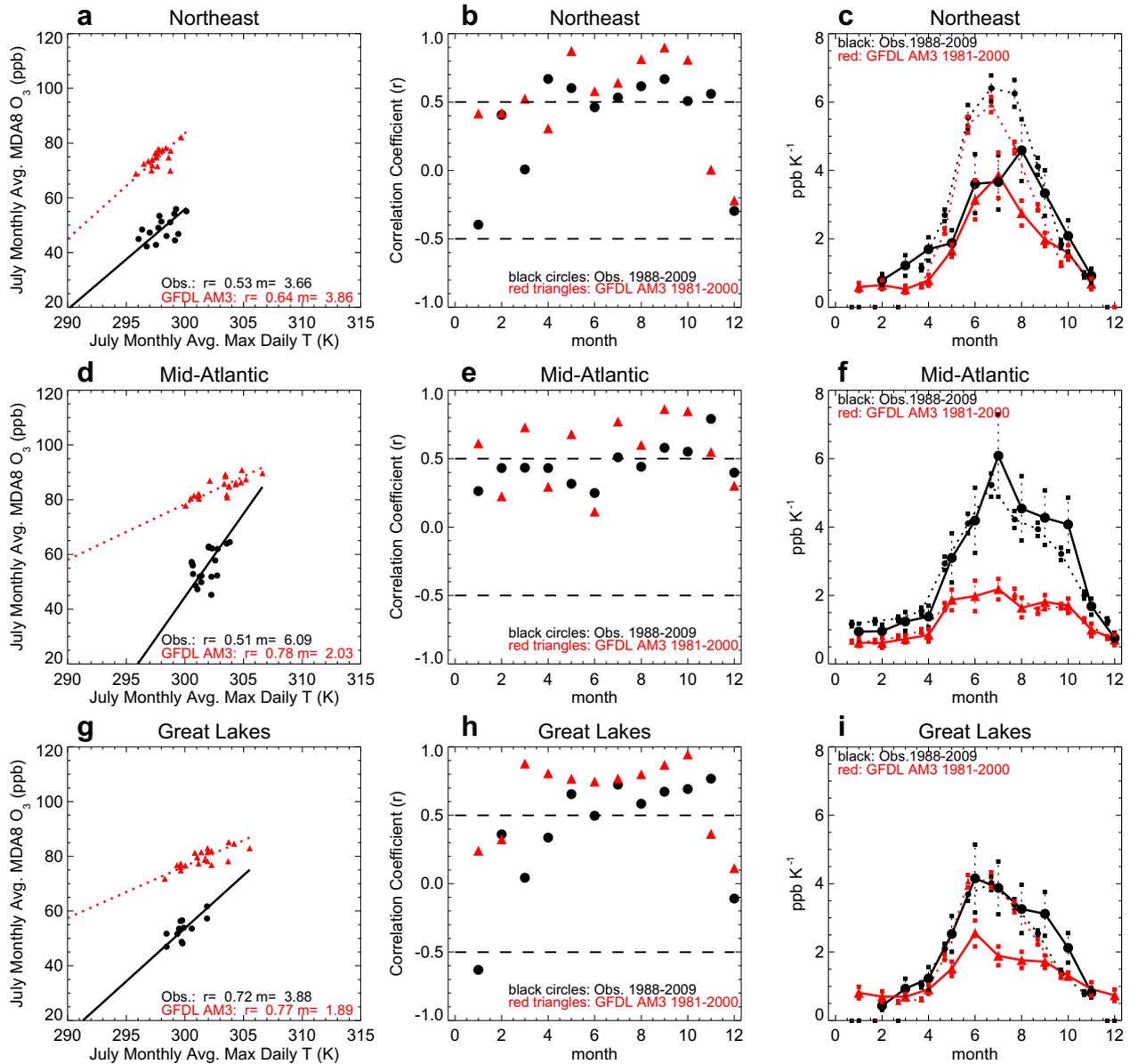
Fig. 6. Relationships between monthly regional averages of MDA8 O_3 (ppb) and of daily T_{max} (K) for individual years from 1988−2009 (solid black circles) and from the GFDL AM3 model for 1981−2000 (red triangles). For each year, we require that 75% of all regional sites within a region for the specified month meet the selection criteria (Section 2); this criteria results in a record length shorter than the full 22 years. Scatter plots of July monthly mean MDA8 O_3 concentration (ppb) and July daily T_{max} (K) with linear regression fits (m_{O3-T}; left column). Also shown are monthly values of Pearson correlation coefficients (r; middle column) and m_{O3-T} (right column); dotted lines use the methodology from Fig. 4 but applied to the full 1988−2009 dataset; m_{O3-T} is not shown for months where $r < 0$; vertical lines indicate ± 1 standard error on m_{O3-T} (ppb K^{-1}). The dashed lines at $r = \pm 0.5$ indicate where at least 25% of the variance in the surface O_3 is associated with temperature variability (For interpretation of the references to color in this figure legend, the reader is referred to the web version of this article.).

over all data modeled at CASTNet site locations within each region to estimate regionally average climatologies (Fig. 6). Despite up to a +10 to +20 ppb O_3 bias, the model captures m_{O3-T} over the Northeast, and with the exception of the timing of the highest m_{O3-T} occurring one month early in the model, the seasonality of m_{O3-T} over the Northeast is generally well simulated (Fig. 6c). Values of m_{O3-T} are also well reproduced in the winter and early spring over the Mid-Atlantic (Fig. 6f) and the Great Lakes (Fig. 6i), but are lower by roughly 2−4 ppb K^{-1} in the Mid-Atlantic and 1−2 ppb K^{-1} in the Great Lakes in the summer (consistent with Figs. 2d and 3d over the Mid-Atlantic) and early autumn. For comparison, the dashed lines in Fig. 6 are monthly values of m_{O3-T} calculated using the methodology from Fig. 4, but extended to the full record length. In the Northeast, we find that the model represents both the spatial

gradients across O_3 and temperature (Fig. 4a−c) as well as the role of year-to-year weather changes on O_3 (Fig. 6a−c). Whereas spatial gradients of O_3 and temperature over the Mid-Atlantic and Great Lakes are well captured by the model (Fig. 4), in these regions the response of O_3 to year-to-year fluctuations in temperature is only weakly reproduced. We find that over these same two regions, monthly mean T_{max} is at times 5 K too warm with respect to the CASTNet sites (Fig. 6d, g). When the modeled monthly mean temperatures that are above the warmest observed monthly mean T_{max} are removed from the data (not shown) over the Mid-Atlantic, a sensitivity of 2.5 ppb K^{-1} is calculated for July ($r = 0.7$). The O_3-temperature sensitivity increases by 5 ppb K^{-1} in the summer months over the Great Lakes when temperatures above 305 K are excluded.
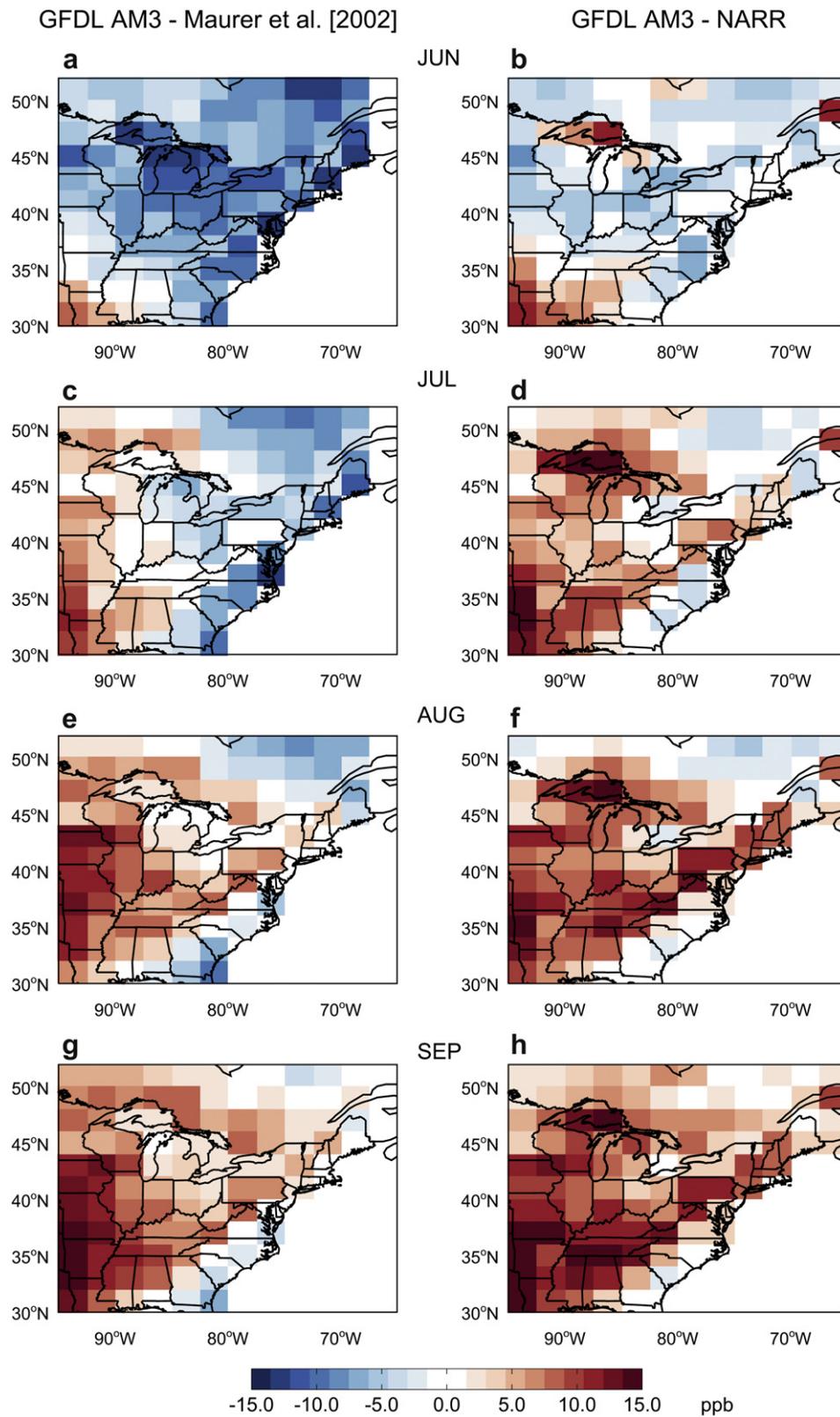
Fig. 7. June, July, August, and September excess modeled O_3 (ppb) attributed to eastern US monthly (1981–2000 average) maximum daily surface temperature biases in the GFDL AM3 CCM; left column uses temperature bias of GFDL AM3 versus Maurer et al. (2002); right column uses bias of GFDL AM3 versus NARR; temperature biases are multiplied by a conservative, observationally-derived estimate for m_{O3-T} for 3 ppb K^{-1} over the eastern US (Figs. 4 and 6).

Fundamentally different meteorological processes modulate O_3 levels in the southern and the northern regions of the eastern US (Camalier et al., 2007). Migratory high-pressure systems strongly influence summer O_3 variability over this domain, except in the south where the stagnant Bermuda high-pressure system tends to limit day-to-day changes (Vukovich, 1995). The model best simulates the O_3-temperature relationship over the Northeast and most of the Great Lakes. In these regions, summertime pollutant ventilation is known to be driven by northeastward propagating cyclones with associated cold fronts extending south to roughly 35° N (Leibensperger et al., 2008; Logan, 1989; Vukovich, 1995); below this latitude, both deep convection and inflow from the Gulf of Mexico have been identified as important pollutant ventilation mechanisms (Li et al., 2005). The better-represented O_3-temperature relationships north versus south of 35° N may indirectly confirm model skill at resolving synoptic scale meteorological systems. In contrast, the lack of skill in the Mid-Atlantic region may point to inadequate representation of both regional circulation and convective ventilation, a notorious problem for global climate models.

A strong linear dependence of O_3 on humidity (anticorrelation) in the southern US has been noted (Camalier et al., 2007; Dawson et al., 2007; Davis et al., 2011). Davis et al. (2011) found the regional model, Community Multiscale Air Quality (CMAQ), to underestimate this predominantly inverse relationship between O_3 and relative humidity over the Mid-Atlantic. A similar problem could be limiting the success of the GFDL AM3 CCM to reproduce observed O_3 levels in this region, though the observed effects of humidity on O_3 have varying sign and have been perceived as slight in comparison to that of temperature (Jacob and Winner, 2009).

5. Estimating the impact of model biases in climatological T_{max} on MDA8 O_3

Excess summertime surface O_3 formation in the eastern US is a pervasive problem in gridded global (Fiore et al., 2009; Murazaki and Hess, 2006; Reidmiller et al., 2009) and regional (Nolte et al., 2008) models and raises questions about the accuracy of their estimates of future O_3 concentrations. Here, we use the O_3-temperature relationship derived from observations (conservatively estimating a 3 ppb K^{-1} sensitivity; Figs. 4c, f, i and 6c, f, i), to investigate the potential contribution of model biases in monthly climatological temperatures to excess surface O_3 over our study domain. To evaluate modeled T_{max} biases where CASTNet sites do not exist, we utilize 20 years (1981–2000) of monthly mean T_{max} from two independent gridded datasets: The University of Washington (UW) (Maurer et al., 2002) and the North American Regional Reanalysis (NARR) (Mesinger et al., 2006). The UW data are hourly observations from the National Oceanic and Atmospheric Administration/National Climatic Data Center Co-op stations spatially interpolated and gridded to $1/8° \times 1/8°$ horizontal resolution. The NARR data are the product of assimilating the NCEP/Department of Energy global reanalysis (Kanamitsu et al., 2002) with a version of the NCEP Eta model at 32 km $\times$ 32 km horizontal resolution.

The estimated impact of the AM3 bias in monthly climatological (1981–2000 average) T_{max} is shown in Fig. 7. Both the NARR and the UW indicate that GFDL AM3 temperatures are too cool in June and thus would act to decrease O_3 levels in this month such that a negative O_3 bias would be expected if temperature biases were the driving factor. In July, the UW temperature record suggests the GFDL AM3 CCM is too cool, yet both the NARR and the CASTNet observations suggest the opposite. The NARR output is 3-hourly while the UW data are calculated from hourly data, so NARR should be inherently cooler than UW; we suggest this discrepancy between the datasets requires additional study.

Given the general rural location of the CASTNet sites in the urbanized eastern US, they may be biased cool (relative to a regional average). The largest model summer T_{max} biases occur over the Great Lakes and the inland Mid-Atlantic. Fig. 7 indicates that these biases for the months of August and September are a possible source of up to 10–15 ppb of the excess modeled O_3, ~30–50% of the O_3 bias in some grid boxes. Since the modeled regional O_3 response to T_{max} in the summer over both the Mid-Atlantic and the Great Lakes is underestimated in the model (Fig. 6f, i), we consider the estimates in Fig. 7 as an upper limit to the contribution of temperature biases to the O_3 bias (using the modeled m_{O3-T} of 2 ppb K^{-1} would lower our estimate to 6–10 ppb). Clearly, excessively warm temperatures are not the only factor contributing to the model O_3 bias as +30 ppb biases occur over some areas with well-simulated T_{max}, particularly in the Mid-Atlantic. Modeled O_3 production chemistry likely contributes; surface O_3 over the eastern US is highly sensitive to the treatment of isoprene nitrate ($RONO_2$) chemistry and whether isoprene nitrates represent a terminal or interim sink for NO_x (Fiore et al., 2005; Horowitz et al., 2007; Ito et al., 2009; Wu et al., 2007).

6. Conclusions

Our study characterizes climatological monthly O_3-temperature relationships from long-term observations over the eastern US for the purpose of evaluating chemistry-climate models (CCMs) that are used to project future air quality. We consider temperature as a proxy to synthesize the complex effects of several temperature-dependent meteorological and chemical processes influencing O_3 concentrations. We report the slope of the O_3-temperature relationship, m_{O3-T}, at both site-level and regional scales, as derived from measurements of monthly mean daily maximum temperatures (T_{max}) and monthly mean daily maximum 8-hour average (MDA8) O_3 concentrations over all available years. By segregating the observations into two time periods (1988–1999 and 2000–2009), we confirm the previously noted ~1 ppb K^{-1} regional decrease in m_{O3-T} between these periods attributed to power plant NO_x emission reductions (Bloomer et al., 2009).

Our evaluation of the GFDL AM3 CCM shows modeled MDA8 O_3 biases in summer (ranging from +10 to +20 ppb in the Northeast and +10 to +30 ppb in the Great Lakes and Mid-Atlantic). Simulated monthly mean T_{max} (1981–2000 average) is at times 5 K too warm with respect to observations in the latter two regions. Despite these biases, GFDL AM3 reproduces the general spatial and temporal characteristics of m_{O3-T} and associated correlation coefficients in the Northeast, although it underestimates m_{O3-T} by 2–4 ppb K^{-1} in the summer over the Mid-Atlantic, where simulated correlation coefficients are weak. The skill of the model in the northern half of the study domain may derive from the ability of the GFDL AM3 CCM to simulate the fundamental meteorological and chemical processes that modulate the surface O_3 response to temperature in that region. These processes include stagnation and ventilation events resulting from migrating synoptic systems across the eastern US (Logan, 1989; Vukovich, 1995; Leibensperger et al., 2008). By contrast, deficient representation of O_3-temperature relationships in the mid-Atlantic may reflect, at least partially, inadequate representation of convection and inflow from the Gulf of Mexico (Li et al., 2005).

We illustrate how the observationally derived O_3-temperature relationships can be applied to estimate the contribution of modeled temperature biases to excess surface O_3 over our study domain. In order to assess model temperature biases over the full domain (rather than solely in the limited locations of the CASTNet sites), we evaluate model monthly (1981–2000 average) T_{max} with two gridded data sets, both of which suggest summer T_{max} biases of up to 5 K

in August and September for the Mid-Atlantic and the Great Lakes. Multiplying these modeled T_{max} biases by our observation-based O_3 sensitivity of 3 ppb K^{-1}, we estimate a maximum contribution of 10–15 ppb O_3 from simulated T_{max} biases, and conclude they are not the major driver of the large-scale O_3 bias.

The larger standard errors in m_{O3-T} calculated from the regionally averaged observed data (Fig. 6) as compared to regional m_{O3-T} constructed from monthly data at each site (Fig. 4) highlights the need for longer data records to improve statistical power and better quantify robust relationships between MDA8 O_3 and T_{max}. As such, we stress the importance of continuing to maintain long-term, quality controlled, co-located meteorology and air quality measurement networks in the eastern US such as that of the CASTNet, for their crucial importance in documenting relationships and trends therein. These observation-derived relationships are fundamentally tied to the meteorological and chemical regimes from which they are derived and thus are not appropriate for projecting future O_3 air quality directly by statistical downscaling from a future temperature distribution. Rather, these observation-based relationships provide useful constraints to evaluate CCM skill at resolving processes relevant to applying CCMs to project the response of air quality to future changes in climate.

Acknowledgements

Appendix. Supplementary materials

An archive of MDA8 O_3-T_{max} statistics, calculated with the methodologies used herein, with measurements from EPA CASTNet sites across the continental US and Alaska are available for download from GFDL/NOAA at http://www.gfdl.noaa.gov/atmospheric-physics-and-chemistry_data.

References

Austin, J., Wilson, R.J., 2006. Ensemble simulations of the decline and recovery of stratospheric ozone. J. Geophys. Res. Atmos. 111.

Aw, J., Kleeman, M.J., 2003. Evaluating the first-order effect of intraannual temperature variability on urban air pollution. J. Geophys. Res. 108, 4365.

Ayers, G.P., 2001. Comment on regression analysis of air quality data. Atmos. Environ. 35, 2423–2425.

Bernard, S.M., Samet, J.M., Grambsch, A., Ebi, K.L., Romieu, I., 2001. The potential impacts of climate variability and change on air pollution-related health effects in the United States. Environ. Health Perspect. 109, 199–209.

Bloomer, B.J., Stehr, J.W., Piety, C.A., Salawitch, R.J., Dickerson, R.R., 2009. Observed relationships of ozone air pollution with temperature and emissions. Geophys. Res. Lett. 36, L09803.

Bloomer, B.J., Vinnikov, K.Y., Dickerson, R.R., 2010. Changes in seasonal and diurnal cycles of ozone and temperature in the eastern US. Atmos. Environ. 44, 2543–2551.

Brühl, C., Crutzen, P.J., 1988. Scenarios of possible changes in atmospheric temperatures and ozone concentrations due to man's activities, estimated with a one-dimensional coupled photochemical climate model. Clim. Dyn. 2, 173–203.

Camalier, L., Cox, W., Dolwick, P., 2007. The effects of meteorology on ozone in urban areas and their use in assessing ozone trends. Atmos. Environ. 41, 7127–7137.

Cantrell, C.A., 2008. Technical Note: review of methods for linear least-squares fitting of data and application to atmospheric chemistry problems. Atmos. Chem. Phys. 8, 5477–5487.

Cardelino, C.A., Chameides, W.L., 1990. Natural hydrocarbons, urbanization, and urban ozone. J. Geophys. Res. Atmos. 95, 13971–13979.

Chan, E., 2009. Regional ground-level ozone trends in the context of meteorological influences across Canada and the eastern United States from 1997 to 2006. J. Geophys. Res. Atmos. 114.

Christensen, J.H., Hewitson, B., Busuioc, A., Chen, A., Gao, X., Held, I., Jones, R., Kolli, R.K., Kwon, W.T., Laprise, R., Rueda, V.M., Mearns, L., Menéndez, C.G., Räisänen, J., Rinke, A., Sarr, A., Whetton, P., 2007. Regional climate projections. In: Climate Change 2007: The Physical Science Basis. Contribution of Working Group I to the Fourth Assessment Report of the Intergovernmental Panel on Climate Change. Cambridge University Press, Cambridge, United Kingdom and New York, NY, USA.

Clark, T.L., Karl, T.R., 1982. Application of prognostic meteorological variables to forecasts of daily maximum one-hour ozone concentrations in the Northeastern United States. J. Appl. Meteorol. 21, 1662–1671.

Clarke, J.F., Edgerton, E.S., Martin, B.E., 1997. Dry deposition calculations for the clean air status and trends network. Atmos. Environ. 31, 3667–3678.

Davis, J., Cox, W., Reff, A., Dolwick, P., 2011. A comparison of CMAQ-based and observation-based statistical models relating ozone to meteorological parameters. Atmos. Environ. 45, 3481–3487.

Davis, J.C., 1986. Statistics and Data Analysis in Geology, second ed. Wiley, New York.

Dawson, J.P., Adams, P.J., Pandis, S.N., 2007. Sensitivity of ozone to summertime climate in the eastern USA: a modeling case study. Atmos. Environ. 41, 1494–1511.

Donner, L.J., Wyman, B.L., Hemler, R.S., Horowitz, L.W., Ming, Y., Zhao, M., Golaz, J.C., Ginoux, P., Lin, S.J., Schwarzkopf, M.D., Austin, J., Alaka, G., Cooke, W.F., Delworth, T.L., Freidenreich, S.M., Gordon, C.T., Griffies, S.M., Held, I.M., Hurlin, W.J., Klein, S.A., Knutson, T.R., Langenhorst, A.R., Lee, H.C., Lin, Y., Magi, B.I., Malyshev, S.L., Milly, P.C.D., Naik, V., Nath, M.J., Pincus, R., Ploshay, J.J., Ramaswamy, V., Seman, C.J., Shevliakova, E., Sirutis, J.J., Stern, W.F., Stouffer, R.J., Wilson, R.J., Winton, M., Wittenberg, A.T., Zeng, F., 2011. The dynamical core, physical parameterizations, and basic simulation characteristics of the atmospheric component AM3 of the GFDL global coupled model CM3. J. Clim. 24, 3484–3519.

Eder, B.K., Davis, J.M., Bloomfield, P., 1993. A characterization of the spatiotemporal variability of non-urban ozone concentrations over the eastern United States. Atmos. Environ. Part A. General Top. 27, 2645–2668.

Emmons, L.K., Walters, S., Hess, P.G., Lamarque, J.F., Pfister, G.G., Fillmore, D., Granier, C., Guenther, A., Kinnison, D., Laepple, T., Orlando, J., Tie, X., Tyndall, G., Wiedinmyer, C., Baughcum, S.L., Kloster, S., 2010. Description and evaluation of the model for ozone and related chemical tracers, version 4 (MOZART-4). Geosci. Model Dev. 3, 43–67.

Fang, Y., Fiore, A.M., Horowitz, L.W., Levy, H., Hu, Y., Russell, A.G., 2010. Sensitivity of the NOy budget over the United States to anthropogenic and lightning NOx in summer. J. Geophys. Res. 115, D18312.

Fiore, A.M., Dentener, F.J., Wild, O., Cuvelier, C., Schultz, M.G., Hess, P., Textor, C., Schulz, M., Doherty, R.M., Horowitz, L.W., MacKenzie, I.A., Sanderson, M.G., Shindell, D.T., Stevenson, D.S., Szopa, S., Van Dingenen, R., Zeng, G., Atherton, C., Bergmann, D., Bey, I., Carmichael, G., Collins, W.J., Duncan, B.N., Faluvegi, G., Folberth, G., Gauss, M., Gong, S., Hauglustaine, D., Holloway, T., Isaksen, I.S.A., Jacob, D.J., Jonson, J.E., Kaminski, J.W., Keating, T.J., Lupu, A., Marmer, E., Montanaro, V., Park, R.J., Pitari, G., Pringle, K.J., Pyle, J.A., Schroeder, S., Vivanco, M.G., Wind, P., Wojcik, G., Wu, S., Zuber, A., 2009. Multimodel estimates of intercontinental source-receptor relationships for ozone pollution. J. Geophys. Res. Atmos. 114.

Fiore, A.M., Horowitz, L.W., Purves, D.W., Levy, H., Evans, M.J., Wang, Y.X., Li, Q.B., Yantosca, R.M., 2005. Evaluating the contribution of changes in isoprene emissions to surface ozone trends over the eastern United States. J. Geophys. Res. Atmos. 110.

Fiore, A.M., Jacob, D.J., Mathur, R., Martin, R.V., 2003. Application of empirical orthogonal functions to evaluate ozone simulations with regional and global models. J. Geophys. Res. Atmos. 108.

Frost, G.J., McKeen, S.A., Trainer, M., Ryerson, T.B., Neuman, J.A., Roberts, J.M., Swanson, A., Holloway, J.S., Sueper, D.T., Fortin, T., Parrish, D.D., Fehsenfeld, F.C., Flocke, F., Peckham, S.E., Grell, G.A., Kowal, D., Cartwright, J., Auerbach, N., Habermann, T., 2006. Effects of changing power plant NOx emissions on ozone in the eastern United States: proof of concept. J. Geophys. Res. Atmos. 111.

Gego, E., Gilliland, A., Godowitch, J., Rao, S.T., Porter, P.S., Hogrefe, C., 2008. Modeling analyses of the effects of changes in nitrogen oxides emissions from the electric power sector on ozone levels in the eastern United States. J. Air Waste Manage. 58, 580–588.

Gego, E., Porter, P.S., Gilliland, A., Rao, S.T., 2007. Observation-based assessment of the impact of nitrogen oxides emissions reductions on ozone air quality over the eastern United States. J. Appl. Meteorol. Clim. 46, 994–1008.

Gilliland, A.B., Hogrefe, C., Pinder, R.W., Godowitch, J.M., Foley, K.L., Rao, S.T., 2008. Dynamic evaluation of regional air quality models: assessing changes in O-3 stemming from changes in emissions and meteorology. Atmos. Environ. 42, 5110–5123.

Godowitch, J.M., Hogrefe, C., Rao, S.T., 2008. Diagnostic analyses of a regional air quality model: changes in modeled processes affecting ozone and chemical-transport indicators from NOx point source emission reductions. J. Geophys. Res. Atmos. 113.

Guenther, A., Karl, T., Harley, P., Wiedinmyer, C., Palmer, P.I., Geron, C., 2006. Estimates of global terrestrial isoprene emissions using MEGAN (Model of Emissions of Gases and Aerosols from Nature). Atmos. Chem. Phys. 6, 3181–3210.

Guenther, A.B., Zimmerman, P.R., Harley, P.C., Monson, R.K., Fall, R., 1993. Isoprene and Monoterpene emission rate variability – model evaluations and sensitivity analyses. J. Geophys. Res. Atmos. 98, 12609–12617.

Hogrefe, C., Lynn, B., Civerolo, K., Ku, J.Y., Rosenthal, J., Rosenzweig, C., Goldberg, R., Gaffin, S., Knowlton, K., Kinney, P.L., 2004. Simulating changes in regional air pollution over the eastern United States due to changes in global and regional climate and emissions. J. Geophys. Res. 109, D22301.

Horowitz, L.W., Fiore, A.M., Milly, G.P., Cohen, R.C., Perring, A., Wooldridge, P.J., Hess, P.G., Emmons, L.K., Lamarque, J.F., 2007. Observational constraints on the chemistry of isoprene nitrates over the eastern United States. J. Geophys. Res. Atmos. 112.

Horowitz, L.W., Walters, S., Mauzerall, D.L., Emmons, L.K., Rasch, P.J., Granier, C., Tie, X., Lamarque, J.F., Schultz, M.G., Tyndall, G.S., Orlando, J.J., Brasseur, G.P., 2003. A global simulation of tropospheric ozone and related tracers: description and evaluation of MOZART, version 2. J. Geophys. Res. 108, 4784.

Ito, A., Sillman, S., Penner, J.E., 2009. Global chemical transport model study of ozone response to changes in chemical kinetics and biogenic volatile organic compounds emissions due to increasing temperatures: sensitivities to isoprene nitrate chemistry and grid resolution. J. Geophys. Res. 114, D09301.

Jacob, D., Horowitz, L.W., Munger, J.W., Heikes, B.G., Dickerson, R.R., Artz, R.S., Keene, W.C., 1995. Seasonal transition from NOx- to hydrocarbon-limited conditions for ozone production over the eastern United States in September. J. Geophys. Res. 100, 9315–9324.

Jacob, D., Logan, J.A., Yevich, R.M., Gardner, G.M., Spivakovsky, C.M., Wofsy, S.C., Munger, J.W., Sillman, S., Prather, M.J., Rodgers, M.O., Westberg, H., Zimmerman, P.R., 1993. Simulation of summertime ozone over North America. J. Geophys. Res. 98, 14797–14816.

Jacob, D., Winner, D.A., 2009. Effect of climate change on air quality. Atmos. Environ. 43, 51–63.

Jaffe, D., 2011. Relationship between surface and free tropospheric ozone in the Western U.S. Environ. Sci. Technol. 45, 432–438.

Kanamitsu, M., Ebisuzaki, W., Woollen, J., Yang, S.K., Hnilo, J.J., Fiorino, M., Potter, G.L., 2002. Ncep-Doe Amip-Ii Reanalysis (R-2). Bull. Am. Meteorol. Soc. 83, 1631–1643.

Kleinman, L.I., 1991. Seasonal dependence of boundary-layer peroxide concentration – the low and high Nox Regimes. J. Geophys. Res. Atmos. 96, 20721–20733.

Klonecki, A., Levy II, H., 1997. Tropospheric chemical ozone tendencies in CO-CH4-NOy-H2O system: their sensitivity to variations in environmental parameters and their application to a global chemistry transport model study. J. Geophys. Res. 102, 21221–21237.

Korsog, P.E., Wolff, G.T., 1991. An examination of urban ozone trends in the Northeastern U.S. (1973–1983) using a robust statistical method. Atmos. Environ. Part B. Urban Atmos. 25, 47–57.

Kunkel, K., Huang, H.C., Liang, X.Z., Lin, J.T., Wuebbles, D., Tao, Z., Williams, A., Caughey, M., Zhu, J., Hayhoe, K., 2008. Sensitivity of future ozone concentrations in the northeast USA to regional climate change. Mitigat. Adapt. Strategies Global Change 13, 597–606.

Lamarque, J.F., Bond, T.C., Eyring, V., Granier, C., Heil, A., Klimont, Z., Lee, D., Liousse, C., Mieville, A., Owen, B., Schultz, M.G., Shindell, D., Smith, S.J., Stehfest, E., Van Aardenne, J., Cooper, O.R., Kainuma, M., Mahowald, N., McConnell, J.R., Naik, V., Riahi, K., van Vuuren, D.P., 2010. Historical (1850–2000) gridded anthropogenic and biomass burning emissions of reactive gases and aerosols: methodology and application. Atmos. Chem. Phys. 10, 7017–7039.

Lamb, B., Guenther, A., Gay, D., Westberg, H., 1987. A national inventory of biogenic hydrocarbon emissions. Atmos. Environ. 21, 1695–1705.

Lawrence, P.J., Chase, T.N., 2007. Representing a new MODIS consistent land surface in the Community Land Model (CLM 3.0). J. Geophys. Res. 112, G01023.

Lehman, J., Swinton, K., Bortnick, S., Hamilton, C., Baldridge, E., Eder, B., Cox, B., 2004. Spatio-temporal characterization of tropospheric ozone across the eastern United States. Atmos. Environ. 38, 4357–4369.

Leibensperger, E.M., Mickley, L.J., Jacob, D.J., 2008. Sensitivity of US air quality to mid-latitude cyclone frequency and implications of 1980–2006 climate change. Atmos. Chem. Phys. 8, 7075–7086.

Levy, J.I., Carrothers, T.J., Tuomisto, J.T., Hammitt, J.K., Evans, J.S., 2001. Assessing the public health benefits of reduced ozone concentrations. Environ. Health Persp. 109, 1215–1226.

Li, Q.B., Jacob, D.J., Park, R., Wang, Y.X., Heald, C.L., Hudman, R., Yantosca, R.M., Martin, R.V., Evans, M., 2005. North American pollution outflow and the trapping of convectively lifted pollution by upper-level anticyclone. J. Geophys. Res. Atmos. 110.

Lin, C.Y.C., Jacob, D.J., Fiore, A.M., 2001. Trends in exceedances of the ozone air quality standard in the continental United States, 1980–1998. Atmos. Environ. 35, 3217–3228.

Lin, X., Trainer, M., Liu, S.C., 1988. On the nonlinearity of the tropospheric ozone production. J. Geophys. Res. Atmos. 93, 15879–15888.

Logan, J.A., 1983. Nitrogen oxides in the troposphere: global and regional budgets. J. Geophys. Res. 88, 10785–10807.

Logan, J.A., 1989. Ozone in rural-areas of the United-States. J. Geophys. Res. Atmos. 94, 8511–8532.

Mahmud, A., Tyree, M., Cayan, D., Motallebi, N., Kleeman, M.J., 2008. Statistical downscaling of climate change impacts on ozone concentrations in California. J. Geophys. Res. 113, D21103.

Maurer, E.P., Wood, A.W., Adam, J.C., Lettenmaier, D.P., Nijssen, B., 2002. A long-term hydrologically based dataset of land surface fluxes and states for the conterminous United States. J. Clim. 15, 3237–3251.

Meinshausen, M., Smith, S., Calvin, K., Daniel, J.S., Kainuma, M.L.T., Lamarque, J.F., Matsumoto, K., Montzka, S.A., Raper, S.C.B., Riahi, K., Thomson, A.M., Velders, G.J.M., van Vuuren, D., 2011. The RCP Greenhouse Gas concentrations and their extension from 1765 to 2300. Clim. Change.

Meleux, F., Solmon, F., Giorgi, F., 2007. Increase in summer European ozone amounts due to climate change. Atmos. Environ. 41, 7577–7587.

Mesinger, F., DiMego, G., Kalnay, E., Mitchell, K., Shafran, P.C., Ebisuzaki, W., Jović, D.A., Woollen, J., Rogers, E., Berbery, E.H., Ek, M.B., Fan, Y., Grumbine, R., Higgins, W., Li, H., Lin, Y., Manikin, G., Parrish, D., Shi, W., 2006. North American regional reanalysis. Bull. Am. Meteorol. Soc. 87, 343–360.

Murazaki, K., Hess, P., 2006. How does climate change contribute to surface ozone change over the United States? J. Geophys. Res. Atmos. 111.

National Research Council (U.S.), Committee on Tropospheric Ozone Formation and Measurement, 1991. Rethinking the Ozone Problem in Urban and Regional Air Pollution. National Academy Press, Washington, DC.

Nolte, C.G., Gilliland, A.B., Hogrefe, C., Mickley, L.J., 2008. Linking global to regional models to assess future climate impacts on surface ozone levels in the United States. J. Geophys. Res. Atmos. 113.

Olszyna, K.J., Luria, M., Meagher, J.F., 1997. The correlation of temperature and rural ozone levels in southeastern USA. Atmos. Environ. 31, 3011–3022.

Putman, W.M., Lin, S., 2007. Finite-volume transport on various cubed-sphere grids. J. Comput. Phys. 227, 55–78.

Racherla, P.N., Adams, P.J., 2006. Sensitivity of global tropospheric ozone and fine particulate matter concentrations to climate change. J. Geophys. Res. 111.

Rayner, N.A., Parker, D.E., Horton, E.B., Folland, C.K., Alexander, L.V., Rowell, D.P., Kent, E.C., Kaplan, A., 2003. Global analyses of sea surface temperature, sea ice, and night marine air temperature since the late nineteenth century. J. Geophys. Res. 108, 4407.

Reidmiller, D.R., Fiore, A.M., Jaffe, D.A., Bergmann, D., Cuvelier, C., Dentener, F.J., Duncan, B.N., Folberth, G., Gauss, M., Gong, S., Hess, P., Jonson, J.E., Keating, T., Lupu, A., Marmer, E., Park, R., Schultz, M.G., Shindell, D.T., Szopa, S., Vivanco, M.G., Wild, O., Zuber, A., 2009. The influence of foreign vs. North American emissions on surface ozone in the US. Atmos. Chem. Phys. 9, 5027–5042.

Sheffield, J., Goteti, G., Wood, E.F., 2006. Development of a 50-year high-resolution global dataset of meteorological forcings for land surface modeling. J. Clim. 19, 3088–3111.

Shevliakova, E., Pacala, S.W., Malyshev, S., Hurtt, G.C., Milly, P.C.D., Caspersen, J.P., Sentman, L.T., Fisk, J.P., Wirth, C., Crevoisier, C., 2009. Carbon cycling under 300 years of land use change: importance of the secondary vegetation sink. Global Biogeochem. Cyc. 23.

Sillman, S., Samson, P.J., 1995. Impact of temperature on oxidant photochemistry in urban, polluted rural and remote environments. J. Geophys. Res. 100, 11497–11508.

Steiner, A.L., Davis, A.J., Sillman, S., Owen, R.C., Michalak, A.M., Fiore, A.M., 2010. Observed suppression of ozone formation at extremely high temperatures due to chemical and biophysical feedbacks. Proc. Natl. Acad. Sci. U.S.A. 107, 19685–19690.

Steiner, A.L., Tonse, S., Cohen, R.C., Goldstein, A.H., Harley, R.A., 2006. Influence of future climate and emissions on regional air quality in California. J. Geophys. Res. 111, D18303.

Vukovich, F.M., 1995. Regional-scale boundary-layer ozone variations in the eastern United-States and their association with meteorological variations. Atmos. Environ. 29, 2259–2273.

Weaver, C.P., Cooter, E., Gilliam, R., Gilliland, A., Grambsch, A., Grano, D., Hemming, B., Hunt, S.W., Nolte, C., Winner, D.A., Liang, X.Z., Zhu, J., Caughey, M., Kunkel, K., Lin, J.T., Tao, Z., Williams, A., Wuebbles, D.J., Adams, P.J., Dawson, J.P., Amar, P., He, S., Avise, J., Chen, J., Cohen, R.C., Goldstein, A.H., Harley, R.A., Steiner, A.L., Tonse, S., Guenther, A., Lamarque, J.F., Wiedinmyer, C., Gustafson, W.I., Leung, L.R., Hogrefe, C., Huang, H.C., Jacob, D.J., Mickley, L.J., Wu, S., Kinney, P.L., Lamb, B., Larkin, N.K., McKenzie, D., Liao, K.J., Manomaiphiboon, K., Russell, A.G., Tagaris, E., Lynn, B.H., Mass, C., Salathé, E., O'Neill, S.M., Pandis, S.N., Racherla, P.N., Rosenzweig, C., Woo, J.H., 2009. A preliminary synthesis of modeled climate change impacts on U.S. regional ozone concentrations. Bull. Am. Meteorol. Soc. 90, 1843–1863.

Wilks, D.S., 2006. Statistical Methods in the Atmospheric Sciences, second ed. Academic Press, Amsterdam, Boston.

Wu, S., Mickley, L.J., Jacob, D.J., Logan, J.A., Yantosca, R.M., Rind, D., 2007. Why are there large differences between models in global budgets of tropospheric ozone? J. Geophys. Res. Atmos. 112.

Wu, S., Mickley, L.J., Leibensperger, E.M., Jacob, D.J., Rind, D., Streets, D.G., 2008. Effects of 2000–2050 global change on ozone air quality in the United States. J. Geophys. Res. 113, D06302.

Wunderli, S., Gehrig, R., 1991. Influence of temperature on formation and stability of surface pan and ozone – a 2-year field-study in Switzerland. Atmos. Environ. Part A. General Top. 25, 1599–1608.

Yienger, J.J., Levy, H., 1995. Empirical-model of global soil-biogenic Nox emissions. J. Geophys. Res. Atmos. 100, 11447–11464.